Optics & Laser Technology 43 (2011) 1420–1423

Contents lists available at ScienceDirect

Optics & Laser Technology

journal homepage: www.elsevier.com/locate/optlastec

Femtosecond laser fabrication of long period fiber gratings and applications in refractive index sensing

Benye Li [a], Lan Jiang [a,*], Sumei Wang [a], Hai-Lung Tsai [b], Hai Xiao [c]

[a] Laser Micro-/Nano-Fabrication Laboratory, School of Mechanical Engineering, Beijing Institute of Technology, 100081, PR China
[b] Laser-Based Manufacturing Laboratory, Department of Mechanical and Aerospace Engineering, Missouri University of Science and Technology (Formerly University of Missouri-Rolla), Rolla, MO 65409, USA
[c] Department of Electrical and Computer Engineering, Missouri University of Science and Technology (Formerly University of Missouri-Rolla), Rolla, MO 65409, USA

ARTICLE INFO

Article history:
Received 1 December 2010
Received in revised form
11 April 2011
Accepted 21 April 2011
Available online 5 May 2011

Keywords:
Femtosecond laser
Long period fiber gratings
Refractive index sensor

ABSTRACT

An improved point-by-point inscription method is proposed to fabricate long period fiber gratings (LPFGs) by using a laser operating at 800 nm with 35 fs duration pulses. The sensitivity to misalignment between the core and the focus is reduced by scanning a rectangular part on the fiber. LPFGs with an attenuation depth of 20 dB are achieved within the wavelength range of 1465–1575 nm. Characterization of the temperature sensitivity and thermal stability of the LPFGs is presented. A 5.6 nm wavelength shift and a 1.2 dB decrease in the attenuation peak are observed following heat treatment at 600 °C for 4 h. The fabricated LPFGs are used as refractive index sensors. The effect of heat treatment on the response of the LPFGs to refractive index changes is also studied.

1. Introduction

Long period fiber gratings (LPFGs) are widely used in optical communications and sensing fields. In sensing fields, LPFGs present obvious advantages such as high sensitivity to temperature and external refractive index changes [1]. Various methods of LPFGs fabrication have been developed, including irradiation by the output from ultraviolet lasers [2,3], and CO_2 lasers [4], exposure to electric arcs [5] and mechanical pressure [6]. Recently, femtosecond lasers have been widely used to fabricate optical devices in transparent materials [7,8].

LPFGs fabricated by an IR (800 nm) femtosecond laser have superior aging characteristics and high resistance to thermal decay [9], but the attenuation depth is only about 8 dB with a relatively large background loss in the irregular spectrum. By controlling the alignment of the focus within the fiber core along the length of the fiber, a more regular transmission spectrum is achieved [10,11]. For the aforementioned IR femtosecond laser inscription method [9–11], the transmission spectrum is very sensitive to the misalignment between the fiber core and the focus of the inscribing beam, which is difficult to control accurately.

The thermal stability and characteristics of LPFGs should be considered when they are used as sensors. The refractive index modulation of the LPFGs will be reduced [12] and the sensitivity to external refractive index changes will be different after heat treatment. A recent paper reports the thermal characteristics of LPFGs with the changes of external refractive indexes [13]. However, the effect of heat treatment on the refractive index (RI) sensing has not been studied.

In this paper, an improved point-by-point inscription method is adopted to reduce the sensitivity to misalignment between the core and the focus by scanning a rectangular part of the fiber. Using this method, LPFGs with the attenuation depths of 20 dB are obtained, which is the highest reported for LPFGs fabricated by IR femtosecond lasers. Characterization of the thermal response and thermal stability of the fabricated LPFGs are presented. The effect of heat treatment on the LPFG refractive index sensitivity is also studied. It is demonstrated that LPFGs fabricated by exposure to the output from femtosecond lasers can be used as refractive index sensors at high temperatures.

2. Experimental setup

A schematic diagram of the experimental setup is shown in Fig. 1. An fs laser (Spectra-Physics) with a pulse width of 35 fs is used to fabricate the LPFG sensors. The center wavelength and repetition rate of the laser are 800 nm and 1 kHz, respectively. A combination of a half-wave plate and a polarizer is used to reduce the laser power, and then several neutral density (ND) filters are used to further reduce the laser power to the desired values.

* Corresponding author. Tel.: +86 10 6891 4517.
E-mail addresses: jianglan@bit.edu.cn, jianglan@mst.edu (L. Jiang).

0030-3992/$ - see front matter © 2011 Elsevier Ltd. All rights reserved.
doi:10.1016/j.optlastec.2011.04.011

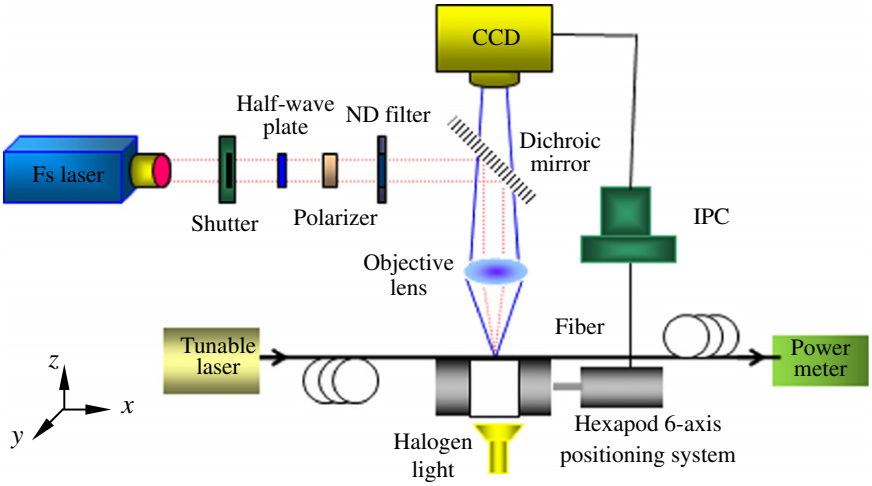

Fig. 1. Schematic diagram of the experimental setup for LPFG fabrication and detection.

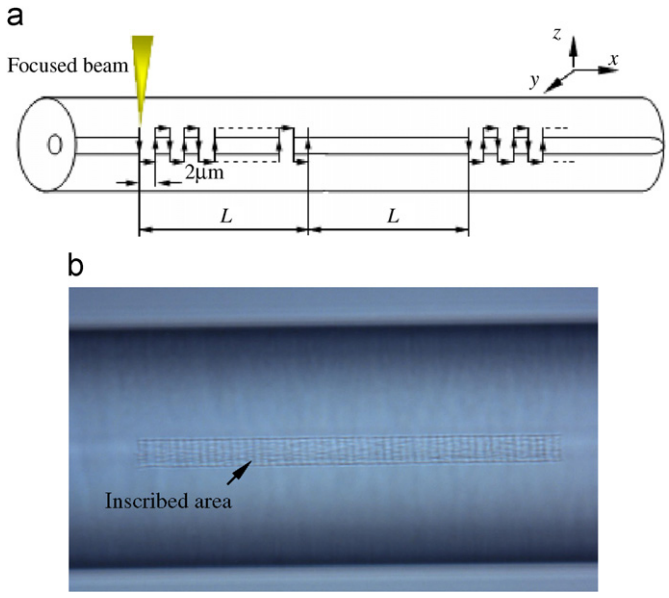

Fig. 2. (a) Beam path during the laser inscribing process and (b) microscope image of an inscribed LPFG.

The laser beam is focused on the fiber core by a 20 × microscopic objective (NA=0.45) and the beam diameter at the focal plan is about 2 μm. The pulse energy is within the range of 0.1–0.5 μJ. The optical fiber used in this experiment is an enhanced telecom fiber SMF-28e (Corning, Inc.) with a core diameter of 8.2 μm, a cladding diameter of 125 μm and a numerical aperture of 0.14. The fiber samples are translated by a 6-axis positioning system with a resolution of 1 μm.

The transmission spectrum of the fiber grating is monitored by the combination of a tunable laser (Agilent81980A, wavelength range 1465–1575 nm) and an optical power meter (Agilent 81636B) during the inscription process. The tunable laser scans through its wavelength range (1465–1575 nm) at the rate of 0.5 nm per step and the power meter detects the power transmitted through the grating.

The polymer coating of the fiber sample is removed and cleaned before the LPFG fabrication. The back-reflected light from the fiber is monitored by a CCD camera and the laser beam is considered to be focused on the center of the fiber core when the image of the back-reflected light becomes a linear shape along the fiber axis [14]. The linear shape would be separated into two parts if there is a deviation between the focal point and the center of the fiber core. The fiber is then moved vertically to the fiber axis away from the center of the fiber core by 8 μm in the focal plane. This position is the actual scanning starting point. The distance of 8 μm is intended to ensure that the scanning area covers the whole fiber core during the fabrication process. Fig. 2 shows the beam path during the laser inscribing process with the step of 2 μm and the microscope image of the fabricated fiber. A rectangular area of $16 \times L$ μm is formed after the laser scanning, where L is half of the grating period (duty ratio is 0.5). The scanning length perpendicular to the axis of the fiber is 16 μm, as compared with the fiber core diameter of 8.2 μm. It ensures that the focused beam scans over the whole fiber core in the y-direction as shown in Fig. 2(a), and reduces the misalignment sensitivity as reported in Ref. [9].

3. Results and discussion

3.1. Effects of pulse energy, grating length and heat treatment on LPFG transmission spectra

During the inscription process, the translation speed, grating period and duty ratio are 50 μm/s, 436 μm and 0.5, respectively. Fig. 3 shows the transmission spectra of LPFGs fabricated with irradiation pulse energies of 0.16, 0.24, 0.32, 0.4 and 0.48 μJ. All gratings have the same length of 25.2 mm. The transmission loss reaches a maximum with the increase in pulse energy (0.16–0.32 μJ), and then declines with further increase in pulse energy (0.32–0.48 μJ). The attenuation band has a red-shift with increasing irradiation fluence, i.e., with the increase in refractive index modulation, which is in agreement with the coupled mode theory [15]. For irradiation pulse energy of 0.32 μJ, the maximum transmission attenuation of 20 dB is obtained at 1525.8 nm and the background loss is only 1 dB. The translation speed is known and the route of scanning path is certain, hence, the time required for each LPFG fabrication can be estimated. It takes about 35 min to process one LPFG.

After the laser beam propagated through a series of optics, the pulse duration is spread to about 50 fs due to the dispersion effects, which is measured before the objective lens. The corresponding ablation threshold fluence of silica is measured to be about 3.6 J/cm^2. However, there isn't a grating signal when the irradiation fluence is 3.6 J/cm^2. Fig. 4 shows the transmission spectra of LPFGs with

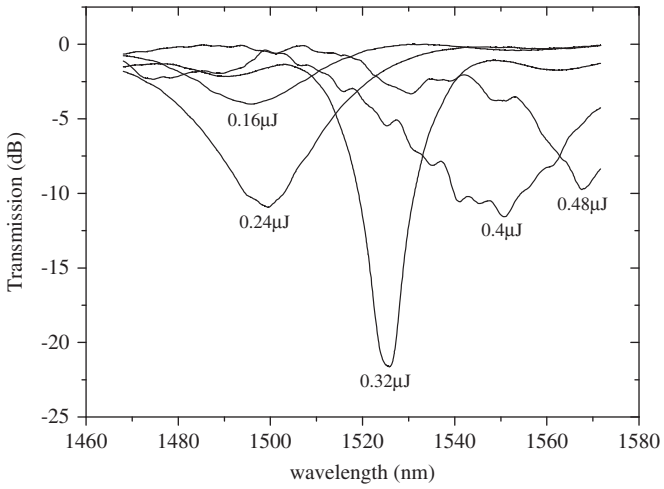

Fig. 3. Transmission spectra of LPFGs fabricated at different laser pulse energies.

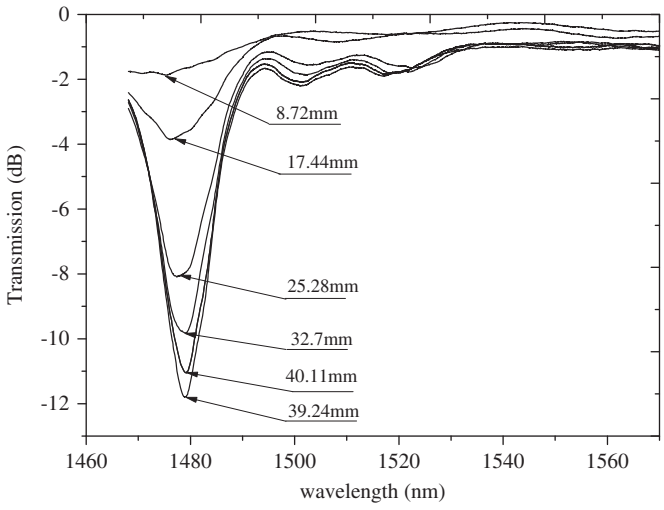

Fig. 4. Transmission spectra of LPFGs with different grating lengths.

different lengths for the same irradiation pulse energy of 0.12 μJ. The corresponding irradiation fluence is 3.8 J/cm^2, a little higher than the ablation threshold fluence. The transmission loss increases with the increase in grating length and reaches maximum with the length of 39.24 mm, while the maximum transmission attenuation is only 10 dB. When the grating length is further increased to 40.11 mm, the attenuation peak begins to decrease for the over-coupling occurs based on the coupled mode theory. Thus, for a given grating period and duty ratio, both the pulse energy and the grating length should be considered during the fabrication process for a high-quality LPFG. The inscription time is about 55 min for the LPFG with a length of 40.11 mm.

During the experiments we also tried to fabricate the LPFGs with various periods in order to achieve significant grating signal in the limited wavelength range of our tunable laser (1465–1575 nm). After many trials, it is found that the maximum attenuation peak is around the center of the wavelength range of the tunable laser with proper pulse energy and grating length when the grating period is 436 μm.

Some regular damage occurred in the cladding area near the incident surface because the used laser fluence was greater than the ablation threshold, as shown in Fig. 2(b). The refractive indices of both the fiber core and cladding are changed after the irradiation, since the energy is absorbed by both the fiber core and cladding [2,3,16]. The details of the refractive index modification are still being investigated by using the plasma model proposed by the authors [17].

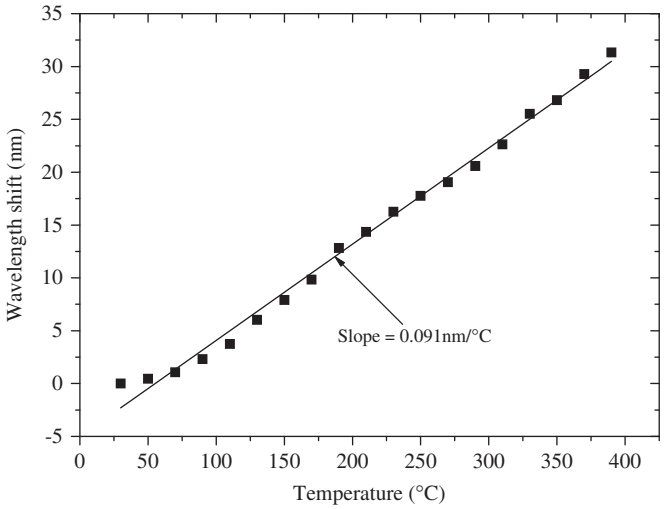

Fig. 5. Resonance wavelength shift of the LPFG versus temperature change.

An LPFG with a length of 25.2 mm is put into an electric Muffle furnace to test the temperature sensitivity. The LPFG has a maximum transmission attenuation of 20 dB around 1525.8 nm. The temperature changed from 30 to 400 °C at a step of 20 °C every 5 min. The peak of the attenuation band has a red-shift when the temperature increases, as shown in Fig. 5. The measured temperature sensitivity is 0.091 nm/°C.

LPFG with background loss of 0.3 dB and attenuation peak around 20 dB is achieved by selecting the appropriate laser fluence and alignment between the inscription focal and the fiber core, as shown in Fig. 6(a). However, background loss always varies from one LPFG to another, because of the motion-stage error, the fiber fabrication error and the laser fluence fluctuations.

An LPFG with background loss around 2 dB is put into the Muffle furnace for 4 h at 600 °C and the background loss is reduced to 0.4 dB after the heat treatment. Furthermore, the heat treatment leads to a 5.6 nm wavelength shift and a 1.2 dB decrease in the attenuation peak, as shown in Fig. 6(b). The highest working temperature of the LPFG inscribed by the fs laser is much higher than that of LPFGs fabricated by157 nm F_2-lasers [3].

3.2. Response to RI changes of the LPFG

The response of a 25-mm-long LPFG to refractive index changes is first investigated without heat treatment. All RI changes tests are at room temperature. The LPFG is fixed on a glass plate to avoid bending-induced signal change. Then, the glass plate is put into different liquids and the transmission spectra are recorded. The liquids are sucrose solution with different concentrations (0%, 30%, 35%, 40%, 45%, 50%, 55% and 60%), and their corresponding RI are 1.3330, 1.3902, 1.3997, 1.4096, 1.4200, 1.4307 and 1.4418, respectively. The device is cleaned by deionized water and air dried after each test of one concentration. The LPFG is put into the Muffle furnace, whose temperature is set at 400 °C for 4 h. After the heat treatment, the LPFG is left at room temperature for 24 h and then the response of the LPFG to RI changes is investigated.

When the surrounding refractive index is changed from n_{ex} to $\overline{n}_{ex}$, the wavelength shift $\delta\lambda_0$ can be expressed as [18]:

$$\delta\lambda_0 \cong \frac{u_\infty^2 \lambda_0^3 \Lambda}{8\pi^3 n_{cl} \rho^3} \left[\frac{1}{\left(n_{cl}^2 - n_{ex}^2\right)^{1/2}} - \frac{1}{\left(n_{cl}^2 - \overline{n}_{ex}^2\right)^{1/2}} \right] \quad (1)$$

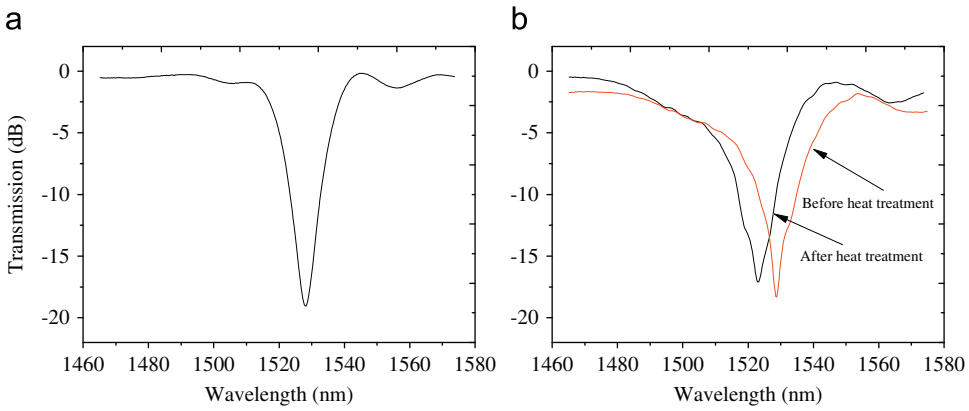

Fig. 6. Transmission spectra of the LPFGs with various background loss: (a) an LPFG with background loss around 0.3 dB and (b) an LPFG with background loss around 2 dB before heat treatment and 0.4 dB after heat treatment.

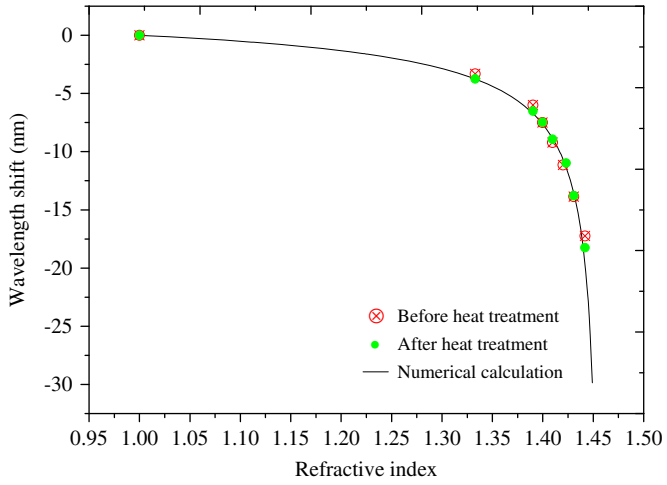

Fig. 7. Wavelength shift as a function of refractive index.

where λ_0 is the resonance wavelength in air, n_{cl} is the cladding refractive index, ρ is the cladding radius, and u_{∞} is the mth root of the Bessel function J_0. Fig. 7 shows the wavelength shift of the LPFG with respect to RI changes. The numerical calculation is based on Eq. (1). A blue-shift is observed in the transmission spectra, which is in good agreement with the numerical calculation. The wavelength shift is more accordant with the numerical calculation curve after the heat treatment. Heat treatment causes a change in refractive index modulation of the grating and more stable grating can be achieved by heat treatment [13]. As a result, the LPFG sensor is more reliable after a proper heat treatment for RI detection.

4. Conclusions

In this study, an improved point-by-point inscription method is developed to make LPFGs with attenuation peak up to 20 dB by using a 800 nm, 35 fs laser. The temperature sensitivity of the LPFG is 0.091 nm/°C and it shows high temperature stability at 600 °C. Theoretically, the LPFG sensors fabricated by our proposed method can stand 1200 °C, which still needs further experimental verification. As an RI sensor, the LPFG becomes more stable after the heat treatment. The results present guidelines to make the LPFGs as temperature sensors and stable refractive index sensors.

Acknowledgments

This research is supported by the National Natural Science Foundation of China (Grant nos. 90923039 and 50705009) and 863 of Ministry of Science and Technology of China (Grant no. 2008AA03Z301).

References

[1] James SW, Tatam RP. Optical fibre long-period grating sensors: characteristics and application. Meas Sci Technol 2003;14:R49–61.
[2] Vengsarkar AM, Lemaire PJ, Judkins JB, Bhatia V, Erdogan T, Sipe JE. Long-period fiber gratings as band-rejection filters. J Lightwave Technol 1996;14(1):58–65.
[3] Chen KP, Herman PR, Zhang J, Tam R. Fabrication of strong long-period gratings in hydrogen-free fibers with 157-nm F_2-laser radiation. Opt Lett 2001;26(11):771–3.
[4] Rao Y-J, Wang Y-P, Ran Z-L, Zhu T. Novel fiber-optic sensors based on long-period fiber gratings written by high-frequency CO_2 laser pulses. J Lightwave Technol 2003;21(5):1320–7.
[5] Hwang IK, Yun SH, Kim BY. Long-period fiber gratings based on periodic microbends. Opt Lett 1999;24(18):1263–5.
[6] Savin S, Digonnet MJF, Kino GS, Shaw HJ. Tunable mechanically induced long-period fiber gratings. Opt Lett 2000;25(10):710–2.
[7] Smelser CW, Mihailov SJ, Grobnic D. Formation of type I-IR and type II-IR gratings with an ultrafast IR laser and a phase mask. Opt Express 2005;13(14):5377–86.
[8] Lin C-H, Jiang L, Xiao H, Chai Y-H, Chen S-J, Tsai. H-L. Fabry–Perot interferometer embedded in a glass chip fabricated by femtosecond laser. Opt Lett 2009;34(16):2408–10.
[9] Kondo Y, Nouchi K, Mitsuyu T, Watanabe M, Kazansky PG, Hirao K. Fabrication of long-period fiber gratings by focused irradiation of infrared femtosecond laser pulses. Opt Lett 1999;24(10):646–8.
[10] Hindle F, Fertein E, Przygodzki C, Durr F, Paccou L, Bocquet R, et al. Inscription of long-period gratings in pure silica and germano–silicate fiber cores by femtosecond laser irradiation. IEEE Photon Technol Lett 2004;16(8):1861–3.
[11] Zhang N, Yang JJ, Wang MW, Zhu XN. Fabrication of long-period fiber gratings using 800 nm femtosecond laser pulses. Chin Phys Lett 2006;23(12):3281–4.
[12] Kalachev AI, Pureur V, Nikogosyan DN. Investigation of long-period fiber gratings induced by high-intensity femtosecond UV laser pulses. Opt Commun 2005;246:107–15.
[13] Costa RZV, Kamikawachi RC, Muller M, Fabris JL. Thermal characteristics of long-period gratings 266 nm UV-point-by-point induced. Opt Commun 2009;282:816–23.
[14] Fujii T, Fukuda T, Ishikawa S, Ishii Y, Sakuma K, Hosoya H. Characteristics improvement of long-period fiber gratings fabricated by femtosecond laser pulses using novel positioning technique. In: Proceedings of the Opt Fiber Commun Conference Los Angeles, CA, USA; 2004, ThC6.
[15] Erdogan T. Cladding-mode resonances in short- and long period fiber grating filters. J Opt Soc Am A 1997;14(8):1760–73.
[16] Slattery SA, Nikogosyan DN. Long-period fiber grating inscription under high-intensity 352 nm femtosecond irradiation: three-photon absorption and energy deposition in cladding. Opt Commun 2005;255:81–90.
[17] Jiang L, Tsai. HL. Plasma modeling for ultrashort pulse laser ablation of dielectrics. J Appl Phys 2006;100:023116.
[18] Chiang KS, Liu Y, Ng MN, Dong X. Analysis of etched long-period fibre grating and its response to external refractive index. Electron Lett 2000;36(17):966–7.